



Article

Commonly Used Therapeutics Associated with Changes in Arousal Inhibit GABA_AR Activation

Anling Kaplan ^{1,†}, Abigail I. Nash ^{2,†}, Amanda A. H. Freeman ^{3,†}, Lauren G. Lewicki ⁴, David B. Rye ⁵, Lynn Marie Trott ⁵, Asher L. Brandt ⁶ and Andrew Jenkins ^{7,*}

- ¹ Department of Anesthesiology, Emory University, Atlanta, GA 30322, USA
² Department of Medical Affairs, Janssen Scientific Affairs LLC, Titusville, NJ 08560, USA
³ Center for Human Health, Emory University, Atlanta, GA 30322, USA
⁴ School of Pharmacy, University of Saint Joseph, West Hartford, CT 06117, USA
⁵ Department of Neurology, Emory University, Atlanta, GA 30322, USA
⁶ Department of Chemistry, University of Saint Joseph, West Hartford, CT 06117, USA
⁷ Department of Pharmaceutical Sciences, University of Saint Joseph, West Hartford, CT 06117, USA
* Correspondence: andrewjenkins@usj.edu
† These authors contributed equally to this work.

Abstract: GABA_A receptor-positive modulators are well-known to induce sedation, sleep, and general anesthesia. Conversely, GABA_A receptor negative allosteric modulators (GABA_ARNAMs) can increase arousal and induce seizures. Motivated by our studies with patients with hypersomnia, and our discovery that two GABA_ARNAMs can restore the Excitation/Inhibition (E/I) balance in vitro and arousal in vivo, we chose to screen 11 compounds that have been reported to modulate arousal, to see if they shared a GABA-related mechanism. We determined modulation with both conventional and microfluidic patch clamp methods. We found that receptor activation was variably modulated by all 11 compounds: Rifampicin (RIF), Metronidazole (MET), Minocycline (MIN), Erythromycin (ERY), Ofloxacin (OFX), Chloroquine (CQ), Hydroxychloroquine sulfate (HCQ), Flumazenil (FLZ), Pentylenetetrazole (PTZ), (-)-Epigallocatechin Gallate (EGCG), and clarithromycin (CLR). The computational modeling of modulator–receptor interactions predicted drug action at canonical binding sites and novel orphan sites on the receptor. Our findings suggest that multiple avenues of investigation are now open to investigate large and brain-penetrant molecules for the treatment of patients with diminished CNS E/I balance.

Keywords: gamma-aminobutyric acid; GABA; GABA_A receptor; GABA_AR; negative allosteric modulator; arousal; sleep; idiopathic hypersomnia



Citation: Kaplan, A.; Nash, A.I.; Freeman, A.A.H.; Lewicki, L.G.; Rye, D.B.; Trott, L.M.; Brandt, A.L.; Jenkins, A. Commonly Used Therapeutics Associated with Changes in Arousal Inhibit GABA_AR Activation. *Biomolecules* **2023**, *13*, 365. <https://doi.org/10.3390/biom13020365>

Academic Editor: Gustav Akk

Received: 15 December 2022

Revised: 7 February 2023

Accepted: 9 February 2023

Published: 15 February 2023



Copyright: © 2023 by the authors. Licensee MDPI, Basel, Switzerland. This article is an open access article distributed under the terms and conditions of the Creative Commons Attribution (CC BY) license (<https://creativecommons.org/licenses/by/4.0/>).

1. Introduction

Synaptic GABA_A receptors (GABA_ARs) are the most common fast inhibitory ligand-gated ion channels in the mammalian central nervous system. The receptors are expressed throughout, with differing spatial and temporal patterns [1]. The heterogeneity of subunit composition and anatomic location bestow divergent patterns of inhibition to various brain regions at different times of development [2]. These patterns of inhibition play a key role in E/I balance. Inherited and de novo mutations that alter receptor function lead to changes in the strength or duration of inhibition, and are associated with many neurologic and psychiatric diseases [3].

The endogenous enhancement of receptor function by steroids and naturally occurring peptides leads to impaired arousal [4,5]. The GABA_A receptor is also a key therapeutic target for many critical therapeutics and clinically useful drugs. Benzodiazepines, Z-drugs, and many general anesthetics all exert their useful actions by positively modulating the GABA_A receptors and mimicking endogenous modulation, resulting in sedation and unconsciousness [6].

Motivated by our discoveries that pathological sleep in humans can be reversed with a benzodiazepine antagonist and a macrolide antibiotic [7–10], we sought to screen commonly used therapeutics that have previously been associated with sleep disruption. Our goal was to discover GABA_AR-NAM activity that may be leveraged to improve arousal in patients with diseases associated with excessive daytime sleepiness.

2. Compounds Tested and Rationale

The molecules tested in this study have previously been associated with neurologic and psychological alterations, and changes in sleep. Rifampicin (RIF) is an antibiotic whose side effect profile includes sedation. Metronidazole (MET) is used to treat anaerobic and protozoal infections, and it is administered orally with a bioavailability >90%. MET reaches 60–100% of plasma concentrations in the CNS, and the pharmacodynamics show activity for 12–24 h after 1 g [11]. MET also has been shown to reduce slow wave sleep (SWS) and increase sleep latency [12]. Minocycline (MIN) is a tetracycline antibiotic that crosses the blood–brain barrier (BBB), and it is used to treat bacterial infections such as pneumonia and respiratory tract infections. MIN has been shown to have anti-inflammatory and neuroprotective functions, and it has been proposed to have a role in treating anxiety and depression [13]. MIN also inhibits protein synthesis, and it appears to reduce SWS [14]. Erythromycin (ERY) is a macrolide antibiotic in the same class as clarithromycin, and it is used to treat and to prevent a wide variety of bacterial infections. In a pilot study in patients suffering from chronic fatigue syndrome, 400 mg ERY altered sleep, possibly due to changes in gut microbiota [15].

Quinolone antibiotics are known to interact directly with the GABA_A receptor. Ofloxacin (OFX) is a fluoroquinolone antibiotic that has been shown to induce hypomania and decrease the need for sleep [16]. OFX shortens sleep time in mice, and it has a dose-dependent psychostimulant effect [17]. OFX has been shown to inhibit the GABA binding in isolated rat neurons in a concentration-dependent manner [18]. Chloroquine (CQ) is used to treat malaria; it has been shown to interact with Cys-loop receptors, and it competitively binds to GABA_ARs [19]. Hydroxychloroquine sulfate (HCQ) is an analog of CQ; it is also used to treat malaria, and it can also act as an anti-inflammatory agent [20]. HCQ is commonly used to treat rheumatoid arthritis, and it is safe for long-term use and has been reported to improve the quality of sleep in patients with primary Sjögren's syndrome who experience a decreased quality of life due to poor sleep quality and excessive daytime sleepiness [21].

Two of the drugs tested here have been used successfully in clinical practice and clinical trials for Idiopathic Hypersomnia (IH). Flumazenil (FLZ) is a GABA_A receptor antagonist that competitively inhibits activity at the benzodiazepine (BZD) site of the GABA_A receptor complex and is FDA approved for the reversal of benzodiazepine-induced sedation. It is believed to antagonize the sedative hypnotic actions of BZDs at the $\gamma\alpha$ subunit interface on GABA_A receptors [7]. Our lab has previously shown that flumazenil acts as a NAM at the GABA_A receptor when activated in the presence of GABA and CSF from hypersomnolent patients. Flumazenil has also had success in the clinical treatment of patients with IH [7,22]. Clarithromycin has been shown to reduce self-reported sleepiness and other disease symptoms in a pilot clinical trial, including participants with IH and other related disorders. Pentylenetetrazole (PTZ) has been previously reported as a GABA antagonist, and it has a long history of clinical use to treat overdoses and psychosis [23]. PTZ has also been shown to be effective in animal models of Down syndrome [24–26], where sleep problems such as excessive daytime sleepiness are common [27]. (-)-Epigallocatechin Gallate (EGCG) is a flavonoid which has been reported to interact with GABA_A receptors, and it can either act as a positive or negative allosteric modulator [28]. It has been reported that low caffeine green tea improves sleep quality and reduces fatigue, based on the fact that caffeine and EGCG suppress the anti-stress effects of theanine [29].

3. Methods

3.1. Molecular Biology and Cell Culture

Human GABA_A receptor cDNAs ($\alpha 1\beta 2\gamma 2s$) were subcloned into the pcDNA 3.1 expression vector, and they were subsequently transfected into HEK293 cells using standard methods. Forty-eight hours later, cells were exposed to individual GABA_A RNAM solutions with simultaneous exposure to GABA. GABA_A RNAMs were obtained from Sigma-Aldrich, and the solutions were prepared with a saline solution to 1–300 μ M concentrations. For rifampicin, 0.5% DMSO was also present in solution for solubility. Stable cell lines were generated and handled as previously described [30].

3.2. Conventional Patch Clamp

Whole-cell recordings—Wild type GABA_A receptors were characterized via whole-cell, voltage-clamp electrophysiology at room temperature 36–72 h after transfection. Patch pipettes were fabricated from thin-walled borosilicate glass (TW150F-4, World Precision Instruments, Inc., Sarasota, FL, USA) using a horizontal puller (P-97, Sutter Instrument Co., Novato, CA, USA). The resistances of the patch pipettes were 2–5 megaohms when filled with an intracellular solution containing 120 mM KCl, 2 mM MgCl₂, 10 mM EGTA, and 10 mM HEPES, adjusted to pH 7.2 with NaOH. Cells were perfused continuously with an extracellular solution containing 160 mM NaCl, 10 mM HEPES, 6 mM D-glucose, 3 mM KCl, 1 mM MgCl₂, and 1.5 mM CaCl₂, adjusted to pH 7.4. Two 10-channel infusion pumps (KD Scientific) and a rapid solution exchanger (Biologic) were used to apply extracellular saline to the cells. Whole-cell currents were recorded at –60 mV, digitized at 100 Hz, and filtered at 50 Hz with a MultiClamp 700B amplifier and a DigiData 1322A interface (Molecular Devices) for offline analysis using bespoke scripts written in MATLAB. The solution changer was driven by protocols written in pClamp 9.2 (Molecular Devices).

3.3. Microfluidic Patch Clamp

Microfluidic electrophysiology: Intracellular saline solutions contained 145 CsCl, 2 CaCl₂, 2 mM MgCl₂, 10 mM EGTA, and 10 mM HEPES. Extracellular saline solutions contained 140 mM NaCl, 5 mM KCl, 2 mM CaCl₂, 1 mM MgCl₂, 10 mM HEPES, and 10 mM D-glucose. Both salines were adjusted to pH 7.4 (330 mOsm) and were 0.2 μ m filter sterilized. The composition was based on solutions designed for long duration HEK293 biophysics studies [31]. HEK293 cells stably expressing mouse $\alpha 1\beta 2\gamma 2L$ receptors [30] were dissociated with detachin (Genlantis, San Diego, CA, USA), resuspended in extracellular saline (2.5×10^6 cells/mL), and agitated prior to loading into 384-well Fluxion ensemble plates. In our hands, these cells can be passaged 3–40 times and still produce reproducible responses to GABA for over 2 years. In addition, we have found that electrophysiology experiments using 30 s episodes are stable and free of rundown for over 45 min. GABA concentration response relationships indicate that 100 μ M GABA elicited >90 % of the maximal response.

Cells were patched using an Ionflux Mercury microfluidic automated patch clamp system [32,33] (Fluxion Biosciences, Oakland, CA, USA). Each experiment ran on a disposable 384-well plate with microfluidic channels printed into an ionized polydimethylsiloxane base. Each plate was divided into 4 zones, each containing 8 repeats of the same experimental pattern (see Figure 1). Each pattern comprised 8 compound wells containing the ligands/modulator combinations to be used in the experiment. Connected to these by a manifold perfusion chamber was an inlet well containing the cell suspension, an outlet well for discarded perfusate, and 2 trapping wells. Both trapping wells contained intracellular solution and were connected to the manifold via 20 1 μ m diameter holes for cell attachment (each pattern can patch up to 40 cells simultaneously). Intracellular electrodes were placed in the 2 trapping wells, and the reference electrode in the waste well. Electrodes were connected to 64 conventional low-noise resistive feedback amplifiers. After cleaning, the plates were loaded with up to 100 μ L of experimental solution or cell suspension per well. Each plate was loaded into the Fluxion Ionflux Mercury device, and a bespoke script

primed the experimental fluidic channels and manifold, and the traps and sealed cells for voltage clamp measurements, and finally, controlled solution application/concentration jumps prior to saving the data collected. Agonist applications were repeated in triplicate (see Supplemental Figure S1). The current data were recorded at 10 kHz and stored for offline analysis. MATLAB scripts were used to measure the baseline leak current and peak response for each episode of data (typically 2000–4000/experiment). The matrix of peaks was expressed as a percentage of the response to a reference concentration. For the agonist concentration–response experiments, this was the maximum response. For the modulator concentration–response experiments, this was the EC₁₀ agonist response.

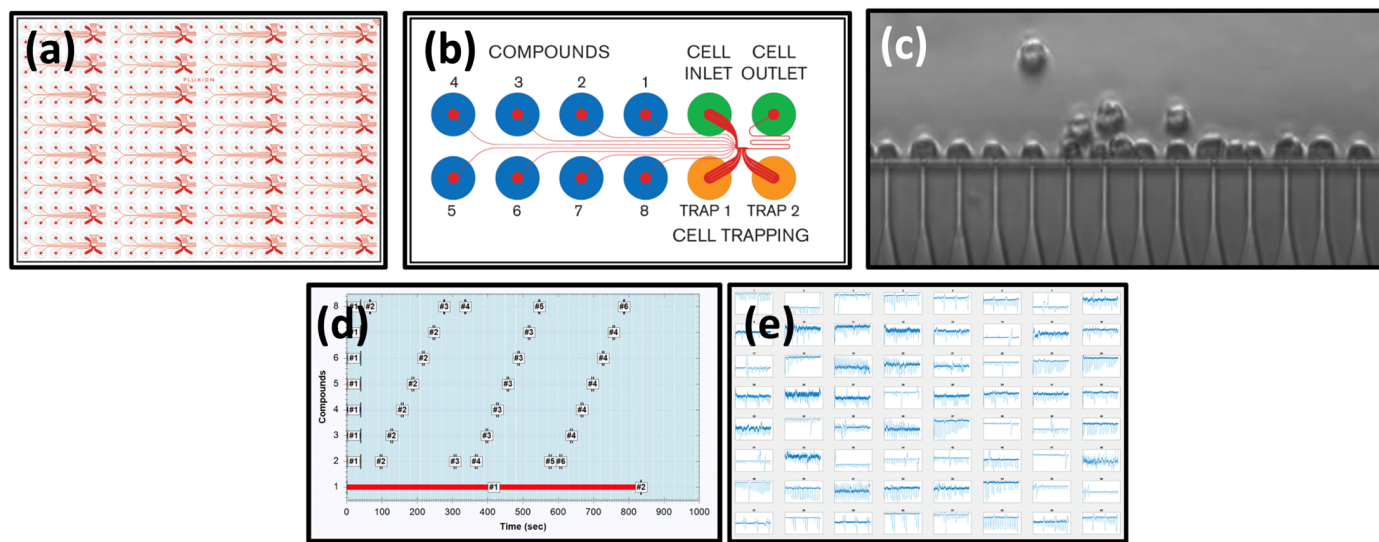


Figure 1. Microfluidic experimental layout. (a) A 384-well HT Mercury plate layout showing 32 repeats of the same perfusion system. The orange color depicts the 12 wells and the microfluidic channels connecting them. (b) Single experimental pattern and microfluidic channels. Compounds are loaded into wells 1–8 (blue), cells are loaded into the inlet and intracellular solutions in the 2 traps well (orange). (c) Fourteen HEK293 cells trapped prior to whole cell seal formation. (d) Eight compounds and nine dose response protocols. (e) Representative data file with 192 dose responses collected in 15 min.

3.4. In Silico Modeling Methods

The published cryo-EM structure (PDB: 6DW0) of the GABA A receptor in complex with GABA was used as a starting template [34]. The 6DW0 was prepared using a protein preparation wizard (Schrödinger, New York, NY, USA), where the bond orders were assigned and the structure was minimized. Each of the structures: chloroquine, erythromycin, metronidazole, minocycline, ofloxacin, (-)-epigallocatechin gallate, flumazenil, hydroxy-chloroquine, pentylenetetrazol, clarithromycin, and rifampicin, were built and optimized in a Spartan '20 Parallel Suite (Wavefunction, Irvine, CA, USA). Tautomers were generated for each ligand, and the dominant ionization states of acidic and basic functional groups were used, assuming pH 7.4 (Schrödinger, New York, NY, USA). QikProp was used to calculate the ADME properties of the 11 ligands tested (Schrödinger, New York, NY, USA). A receptor grid generator was used to place $10 \text{ \AA} \times 10 \text{ \AA} \times 10 \text{ \AA}$ boxes covering the whole receptor (Schrödinger, New York, NY, USA). All 11 ligands were run for each of the grid boxes generated in Glide SP, using flexible docking with enhanced conformational sampling by four-fold, and an expanded sampling for the selection of initial poses (Schrödinger, New York, NY, USA). The binding site for each ligand was chosen based on the most negative glide score. Erythromycin was not found to bind to any of the sites, and thus it was not carried forward. For each ligand–receptor complex, a minimization was run to reduce steric clashing between the ligand–receptor complex (Schrödinger, New York,

NY, USA) using the VGSB solvation model. MMGBSA was run on each ligand–receptor complex to determine their relative affinities.

4. Results

4.1. Electrophysiology

First, guided by our clinical experience, we investigated whether clarithromycin could reverse the CSF-induced enhancement of the GABA receptor function, as we have previously shown with flumazenil [7]. Using a conventional single electrode patch clamp, we found that CSF from hypersomnolent patients enhanced GABA by $89 \pm 11\%$ ($n = 6$ cells). Clarithromycin reversed this potentiation by $71 \pm 13\%$ ($n = 6$ cells, see Figure 2a). However, unlike flumazenil, we observed that clarithromycin was also able to inhibit GABA_A receptor activation (Figure 2b), revealing that unlike flumazenil’s benzodiazepine antagonist actions, clarithromycin acts as a GABA_A receptor negative allosteric modulator or a GABA antagonist. Next, we chose to replicate this finding using a high throughput microfluidic patch clamp assay. We found this technique readily reproduced our previous finding, validating it as a suitable replacement for the traditional low-throughput technique. Using the ion flux system, we determined that clarithromycin reversibly inhibited GABA_A receptor activation in a concentration-dependent manner up to $300 \mu\text{M}$ (see Figure 3). Next, we sought to further validate our microfluidic method using the well-established GABA_A RNAM pentylenetetrazole (PTZ). Again, we were able to demonstrate that this method was well-suited to measuring GABA_A receptor modulation, and reproduced previous findings, showing that PTZ blocked GABA_AR activation in a concentration-dependent manner (see Figure 4 and Table 1). Next, we determined the effect of ofloxacin on GABA_AR activation using both electrophysiologic techniques. In both cases, we found that ofloxacin produced a modest and incomplete block of receptor activation (see Figure 5 and Table 1). Similarly, we found that chloroquine and hydroxychloroquine exhibited a modest and incomplete block of receptor activation at the highest concentrations used (see Figure 6 and Table 1). Finally, using only the microfluidic method, we similarly found that metronidazole and EGCG produced a modest inhibition of GABA activation (see Figures 7 and 8 and Table 1).

Table 1. Clinical and physiologic parameters for 10 compounds studied with GABA_A receptors in this study. Concentrations are given in μM . Data are mean \pm standard error of the mean for 20–24 determinations. [CNS] denotes concentration of drug in the CNS. I_{max}(%) denotes maximum inhibition.

| Drug | Class | Use | [CNS] | GABA EC ₅₀ | I _{max} (%) | n _H |
|--------------------|----------------|----------------------|-----------|-----------------------|----------------------|----------------|
| EGCG | polyphenol | dietary supplement | 0.18 [35] | 31 ± 4 | 22 ± 8 | 1.1 |
| Chloroquine | aminoquinolone | antimalarial | 1.60 [36] | | | |
| Clarithromycin | macrolide | antibiotic | 10 [37] | 20 ± 1 | 85 ± 8 | 1 |
| Erythromycin | macrolide | antibiotic | 0.68 [38] | | | |
| Hydroxychloroquine | aminoquinolone | antimalarial | 50 [39] | 40 ± 8 | 29 ± 4 | 1.4 |
| Metronidazole | nitroimidazole | Antibiotic/protozoal | 7010 [40] | 50 ± 11 | 24 ± 9 | 0.8 |
| Minocycline | tetracycline | antibiotic | 1.1 [41] | | | |
| Ofloxacin | quinolone | antibiotic | 5.6 [42] | 15 ± 4 | 61 ± 7 | 1 |
| pentylenetetrazole | azepine | stimulant/convulsant | 330 [43] | 10 ± 3 | 68 ± 5 | 1.3 |
| Rifampin | ansamycin | antibiotic | 3.60 [44] | | | |

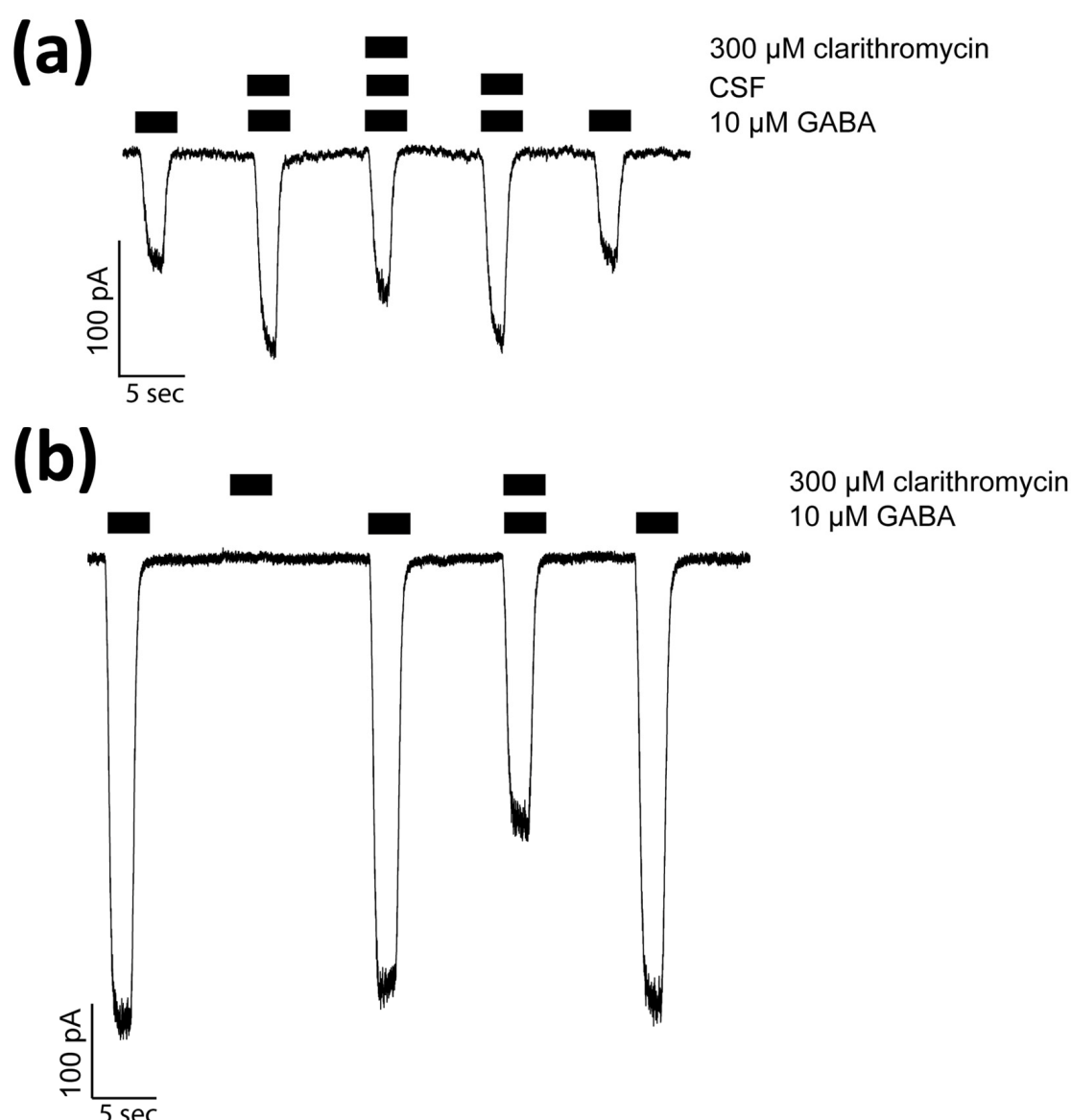


Figure 2. Clarithromycin inhibits CSF-mediated GABA receptor potentiation and activation. Whole cell voltage clamp recordings from HEK293 cells expressing $\alpha 1\beta 2\gamma 2s$ GABA_ARs. **(a)** CSF from a patient diagnosed with Idiopathic Hypersomnia reversibly enhances/potentiates currents activated by 10 μ M GABA (EC₁₀). The potentiation is reduced in the presence of 300 μ M clarithromycin. **(b)** Clarithromycin has no intrinsic efficacy at GABA_A receptor, but reversibly inhibits receptor activation. Bars above the current traces indicate the duration of agonist/modulator application. Calibration bars indicate current amplitude and duration in pA and seconds.

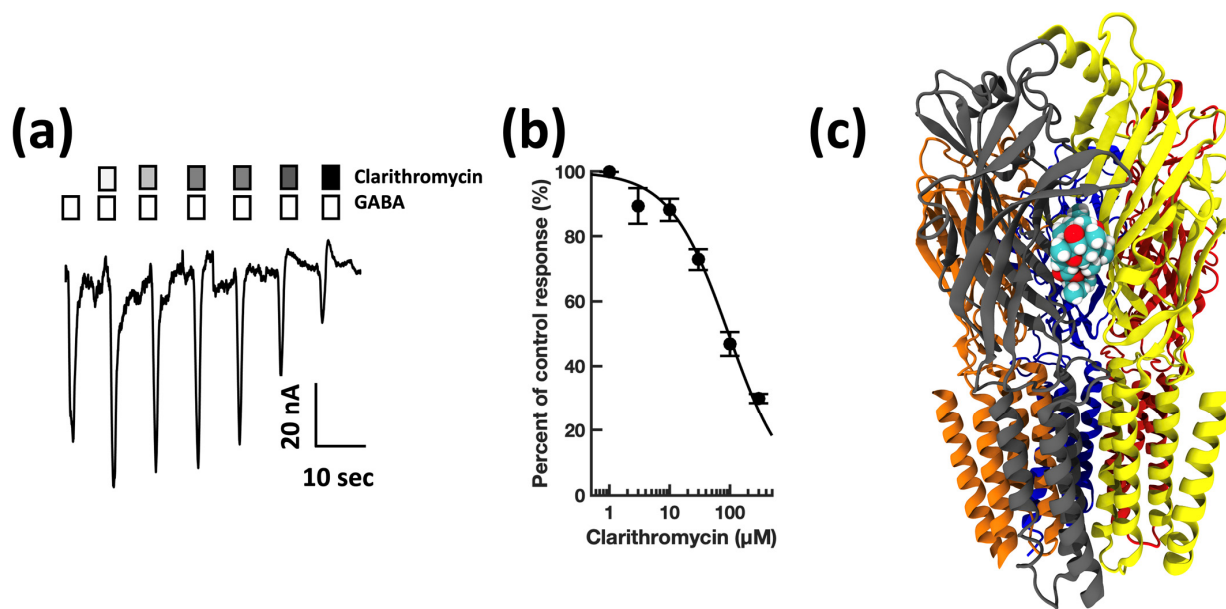


Figure 3. Clarithromycin inhibits GABA_A receptor activation in a concentration-dependent manner, and preferentially docks at the $\alpha + \beta$ -Interface in a pocket defined by canonical loops A-F. (a) Representative microfluidic ensemble whole cell recording from HEK293 cells expressing rat $\alpha 1\beta 2\gamma 2s$ GABA_A receptors. Open bars above the current trace indicate the duration of GABA application. Shaded bars indicate the duration of clarithromycin application. Darker shading indicates increased concentration. The concentrations applied were 1, 3, 10, 30, 100, and 300 μ M clarithromycin. Calibration bars indicate the current amplitude and duration in nA and seconds. (b) Clarithromycin concentration response relationship for GABA receptor modulation. Each point is plotted as mean \pm standard error of the mean for 20–24 determinations. (c) The clarithromycin binding pocket is predicted to be defined by the α (loops A and C, and the $\beta 1\beta 2$ turn) and β (Loops D, F) subunits. Color key: α subunit (red and grey), β subunit (yellow and orange), γ subunit (blue).

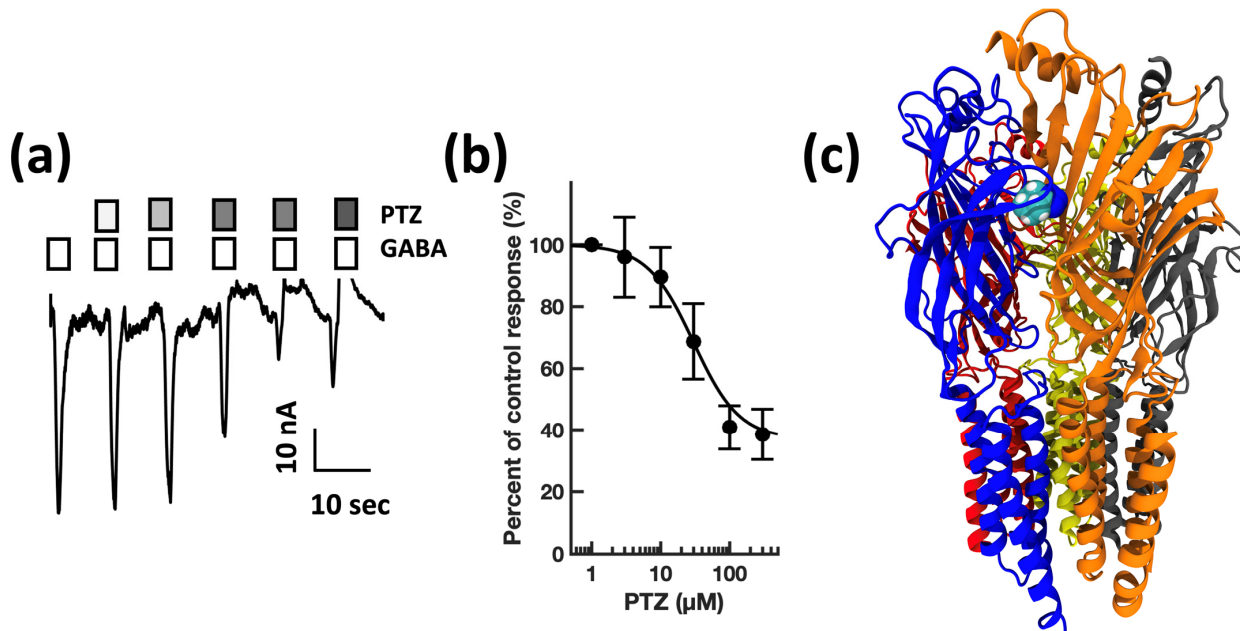


Figure 4. Pentylenetetrazole inhibits GABA_A receptor activation in a concentration-dependent manner, and preferentially docks at the $\gamma + \beta$ Interface in a pocket defined by canonical loops A-E. (a) Representative microfluidic ensemble whole cell recording from HEK293 cells expressing rat

$\alpha 1\beta 2\gamma 2s$ GABA_A receptors. Open bars above the current trace indicate the duration of GABA application. Shaded bars indicate the duration of pentylenetetrazole application. Darker shading indicates increased concentration. The concentrations applied were 1, 3, 10, 30, and 100 μ M pentylenetetrazole. Calibration bars indicate current amplitude, and duration in nA and seconds. (b) Pentylenetetrazole concentration response relationship for GABA receptor modulation. Each point is plotted as mean \pm standard error of the mean for 20–24 determinations. (c) The pentylenetetrazole binding pocket is predicted to be defined by the γ (loops D and E) and β (Loops A, B, and C) subunits. Color key: α subunit (red and grey), β subunit (yellow and orange), γ subunit (blue).

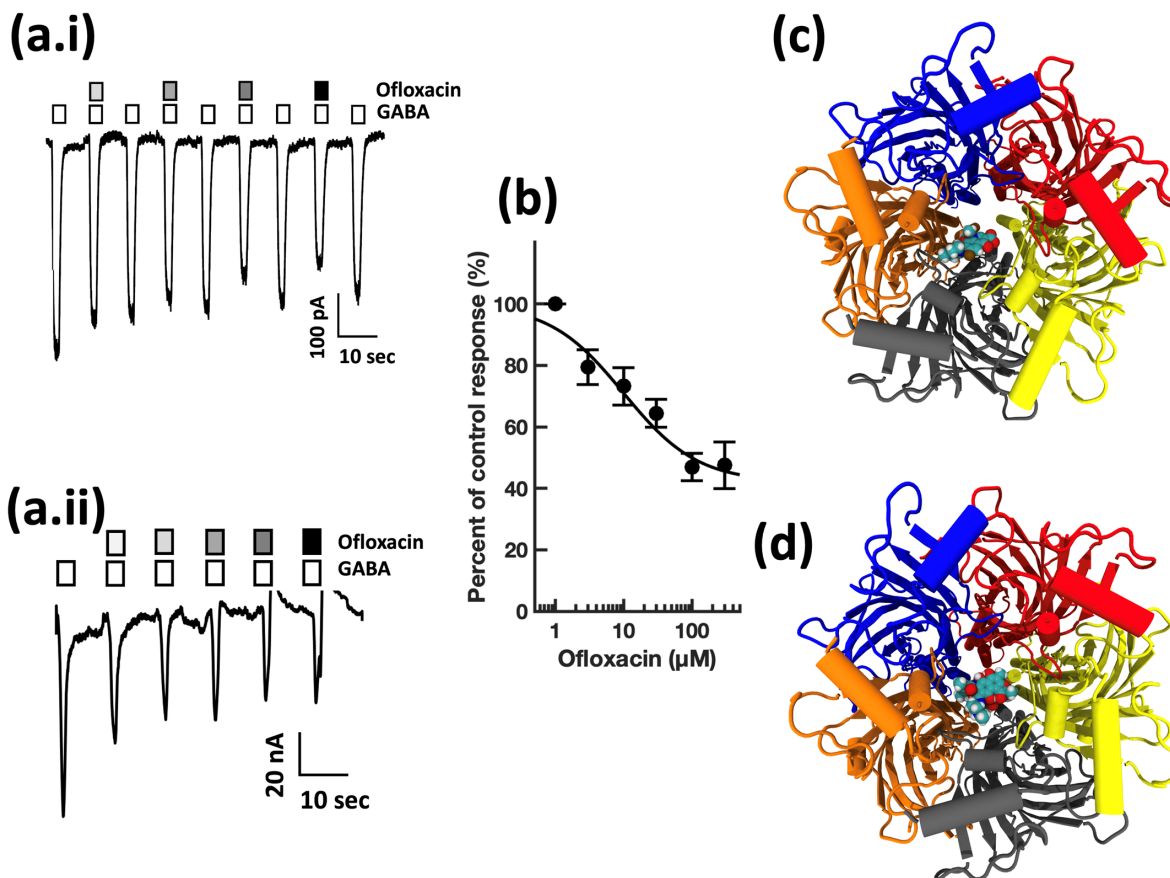


Figure 5. Ofloxacin inhibits GABA_A receptor activation in a concentration-dependent manner, and preferentially docks in the channel lumen at a location shared by rifampicin. (a.i) Conventional single electrode whole cell voltage clamp recording from a HEK293 cell expressing human $\alpha 1\beta 2\gamma 2s$ GABA_ARs. Open bars above the current trace indicate the duration of GABA application. Shaded bars indicate the duration of ofloxacin application. Darker shading indicates increased concentration. The concentrations applied were 1, 3, 10, 30 μ M ofloxacin. Calibration bars indicate current amplitude and duration in pA and seconds. (a.ii) Representative microfluidic ensemble whole cell recording from HEK293 cells expressing rat $\alpha 1\beta 2\gamma 2s$ GABA_A receptors. Open bars above the current trace indicate the duration of GABA application. Shaded bars indicate the duration of ofloxacin application. Darker shading indicates increased concentration. The concentrations applied were 3, 10, 30, 100, and 300 μ M ofloxacin. Calibration bars indicate current amplitude, and duration in nA and seconds. (b) Ofloxacin concentration response relationship for GABA receptor modulation. Each point is plotted as mean \pm standard error of the mean for 20–24 determinations. (c) The ofloxacin binding pocket is predicted to be defined by the lumen-facing residues of the BAE chains ($\beta\alpha\beta$ subunits). (d) The rifampicin binding pocket is predicted to be defined by lumen-facing residues of the BAED chains ($\beta\alpha\beta\gamma$ subunits). Color key: α subunit (red and grey), β subunit (yellow and orange), γ subunit (blue).

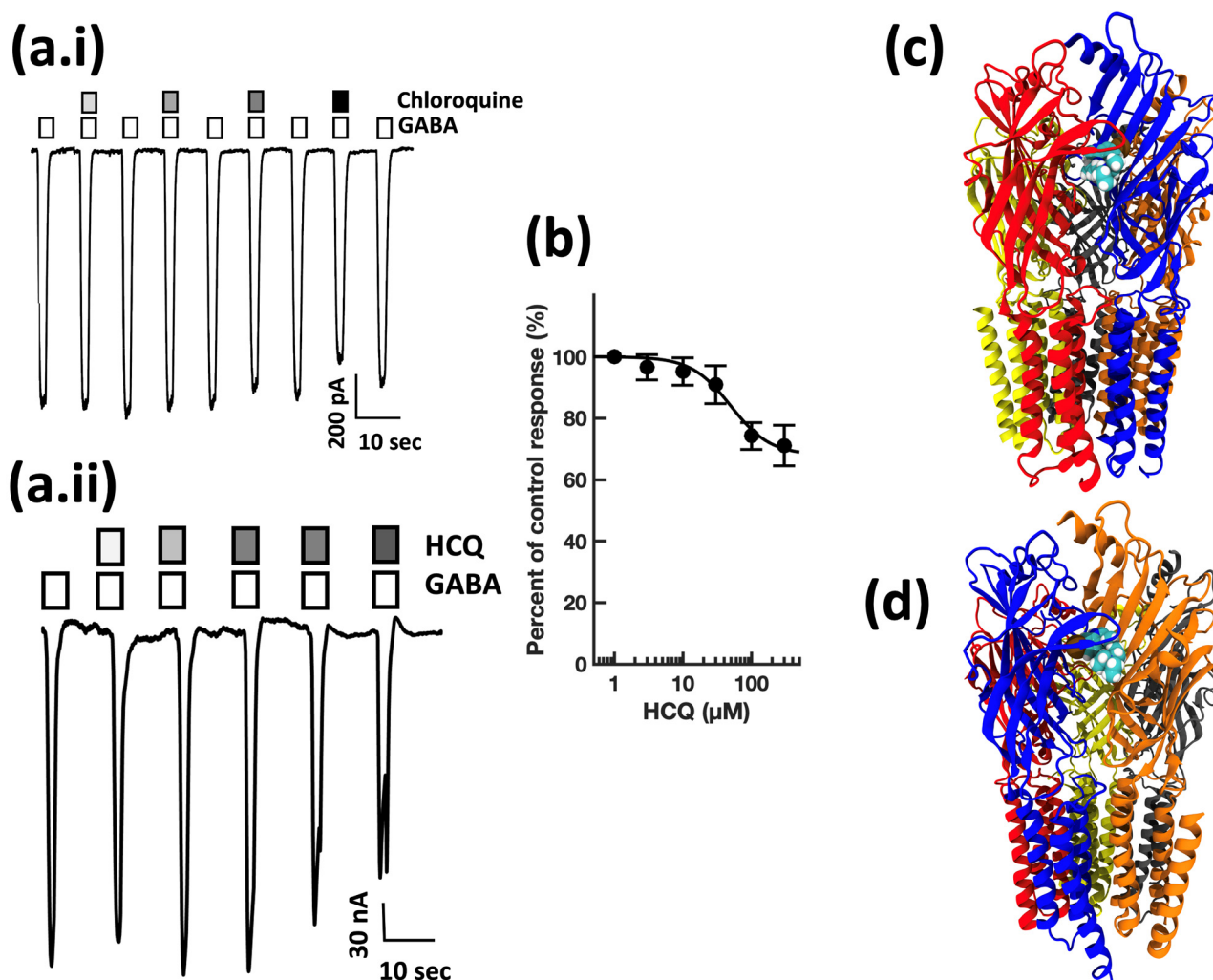


Figure 6. Chloroquine and hydroxychloroquine inhibit GABA_A receptor activation in a concentration-dependent manner, and dock to pockets on the γ subunit. (a.i) Conventional single electrode whole cell voltage clamp recording from a HEK293 cell expressing human $\alpha 1\beta 2\gamma 2s$ GABA_ARs. Open bars above the current trace indicate the duration of GABA application. Shaded bars indicate the duration of chloroquine application. Darker shading indicates increased concentration. The concentrations applied were 1, 3, 10, and 30 μ M chloroquine. Calibration bars indicate current amplitude, and duration in pA and seconds. (a.ii) Representative microfluidic ensemble whole cell recording from HEK293 cells expressing rat $\alpha 1\beta 2\gamma 2s$ GABA_A receptors. Open bars above the current trace indicate the duration of GABA application. Shaded bars indicate the duration of hydroxychloroquine application. Darker shading indicates increased concentration. The concentrations applied were 3, 10, 30, 100, and 300 μ M hydroxychloroquine. Calibration bars indicate current amplitude and duration in nA and seconds. (b) Hydroxychloroquine concentration response relationship for GABA receptor modulation. Each point is plotted as mean \pm standard error of the mean for 20–24 determinations. (c) The chloroquine binding pocket is predicted to be defined by the α (Loops A, B, and C) and γ (Loops D, E, and F) subunits, overlapping with the canonical benzodiazepine binding site. (d) The hydroxychloroquine binding pocket is predicted to be defined by the β (loops D, E, and F) and γ (loops A, B, and C) subunits. Color key: α subunit (red and grey), β subunit (yellow and orange), γ subunit (blue).

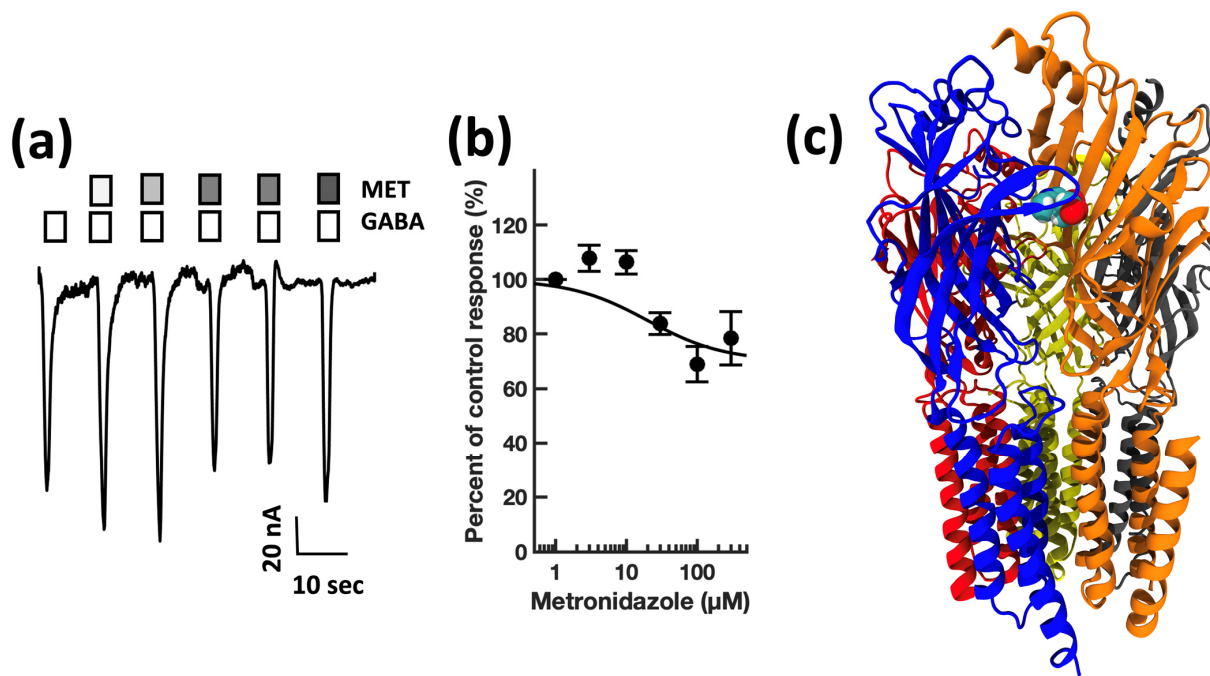


Figure 7. Metronidazole modestly inhibits GABA_A receptor activation in a concentration-dependent manner, and preferentially docks at the $\gamma + \beta$ —Interface in a pocket defined by canonical loops A–E. (a) Representative microfluidic ensemble whole cell recording from HEK293 cells expressing rat $\alpha 1\beta 2\gamma 2s$ GABA_A receptors. Open bars above the current trace indicate the duration of GABA application. Shaded bars indicate the duration of metronidazole application. Darker shading indicates increased concentration. The concentrations applied were 3, 10, 30, 100, and 300 μ M metronidazole. Calibration bars indicate the current amplitude and duration in nA and seconds. (b) Metronidazole concentration response relationship for GABA receptor modulation. Each point is plotted as mean \pm standard error of the mean, for 20–24 determinations. (c) The metronidazole binding pocket is predicted to be defined by the β (loops D, E, and F) and γ (Loops B and C) subunits. Color key: α subunit (red and grey), β subunit (yellow and orange), γ subunit (blue).

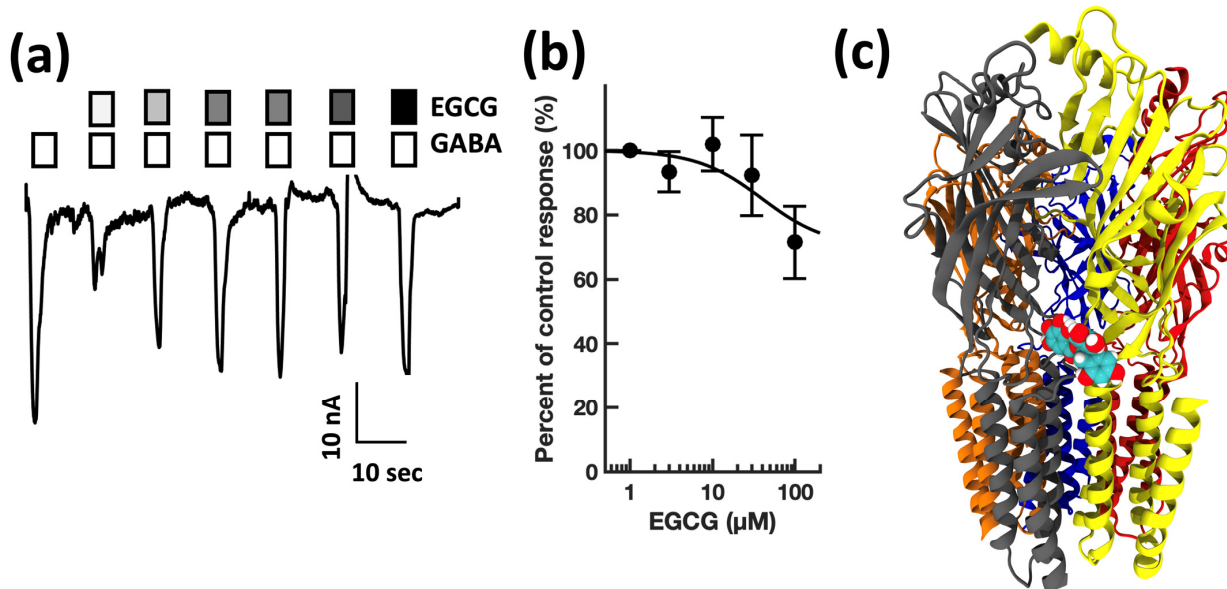


Figure 8. EGCG modestly inhibits GABA_A receptor activation in a concentration-dependent manner, and preferentially docks at the $\alpha + \beta$ Interface in a pocket defined by a TM23 linker, a cys-loop, and

one loop F. (a) Representative microfluidic ensemble whole cell recording from HEK293 cells expressing rat $\alpha 1\beta 2\gamma 2s$ GABA_A receptors. Open bars above the current trace indicate the duration of GABA application. Shaded bars indicate the duration of EGCG application. Darker shading indicates increased concentration. The concentrations applied were 1, 3, 10, 30, 100, and 300 μ M EGCG. Calibration bars indicate current amplitude and duration in nA and seconds. (b) EGCG concentration response relationship for GABA receptor modulation. Each point is plotted as mean \pm standard error of the mean for 20–24 determinations. (c) The EGCG binding pocket is predicted to be defined by the α (TM23 linker and the cys-loop) and β (Loop F) subunits. Color key: α subunit (red and grey), β subunit (yellow and orange), γ subunit (blue).

4.2. Modeling

First, for our docking studies, we did not preselect any candidate binding sites or pockets, nor did we bias our results by choosing specific binding sites for each compound. Instead, we used the comprehensive method described above to find the best score for each ligand–receptor pair throughout the whole receptor. To validate our methodology, we first docked flumazenil to the 6DW0.PDB GABA_A receptor structure. We were pleased when our method predicted that flumazenil binds to the $\alpha^+\gamma^-$ canonical benzodiazepine binding site, where it is known to interact [45], validating our approach (see Supplemental Figure S2).

Next, our docking studies predicted that the 8/9 of molecules under investigation could bind one of four distinct binding pockets in the 6DW0.pdb model of the rat $\alpha 1\beta 1\gamma 2s$ receptor. The only exception was erythromycin, which failed to interact with the model. We found that none of the compounds located into either of the two canonical GABA $\beta^+\alpha^-$ binding sites, or any of the transmembrane anesthetic binding pockets. Our docking studies predicted that chloroquine, like flumazenil, can locate in the $\alpha^+\gamma^-$ benzodiazepine binding site (see Figure 6c). Next, we found that ofloxacin and rifampicin can bind to the central axial extracellular lumen between the five subunits (see Figure 5c,d). Clarithromycin preferentially docks to the $\alpha^+\beta^-$ cavity that until recently was thought to be an orphan homologue of the two $\beta^+\alpha^-$ GABA binding sites (see Figure 3c). However, this view has recently been challenged, and this site has been proposed to be a third GABA binding site [34]. We found that EGCG also docked at this interface, but closer to the transmembrane region where it can interact with residues in the cys-loop and the TM23 linker. Finally, the orphan binding pocket at the $\gamma^+\beta^-$ interface is predicted to interact with MIN, HCQ, MET, and PTZ (see Figures 6d, 7c and 4c). This latter finding is particularly interesting, since despite its long clinical use and known interactions with GABA_A receptors, no binding site has been proposed for PTZ. The in silico modeling parameters determined in this study are shown in Table 2, and the different docking site locations are summarized in Figure 9.

Table 2. In silico modeling parameters for docking 11 compounds to the 6DW0.pdb GABA_A receptor structure.

| Compound | Glide Score | MMGBSA | QPlogPo/w | QPlogkhsa | CNS |
|-----------------------------|-------------|--------|-----------|-----------|-----|
| Chloroquine | -9.528 | -69.04 | 4.653 | 0.629 | 1 |
| Erythromycin | N/A | N/A | 2.558 | -0.060 | -1 |
| Metronidazole | -6.505 | -38.49 | -0.019 | -0.688 | -2 |
| Minocycline | -6.690 | -47.42 | 0.323 | 0.178 | -2 |
| Ofloxacin | -4.224 | -30.44 | -0.388 | -0.431 | 0 |
| (-)Epigallocatechin gallate | -10.319 | -65.68 | -0.275 | -0.447 | -2 |
| Flumazenil | -9.324 | -44.59 | 1.956 | -0.442 | 0 |
| Hydroxychloroquine | -10.956 | -65.90 | 3.564 | 0.207 | 1 |
| Pentylenetetrazol | -6.954 | -33.85 | 0.555 | -0.658 | 0 |
| Clarithromycin | -3.271 | -34.09 | 3.090 | 0.058 | 0 |
| Rifampicin | -3.052 | -41.18 | 3.302 | -0.181 | -2 |

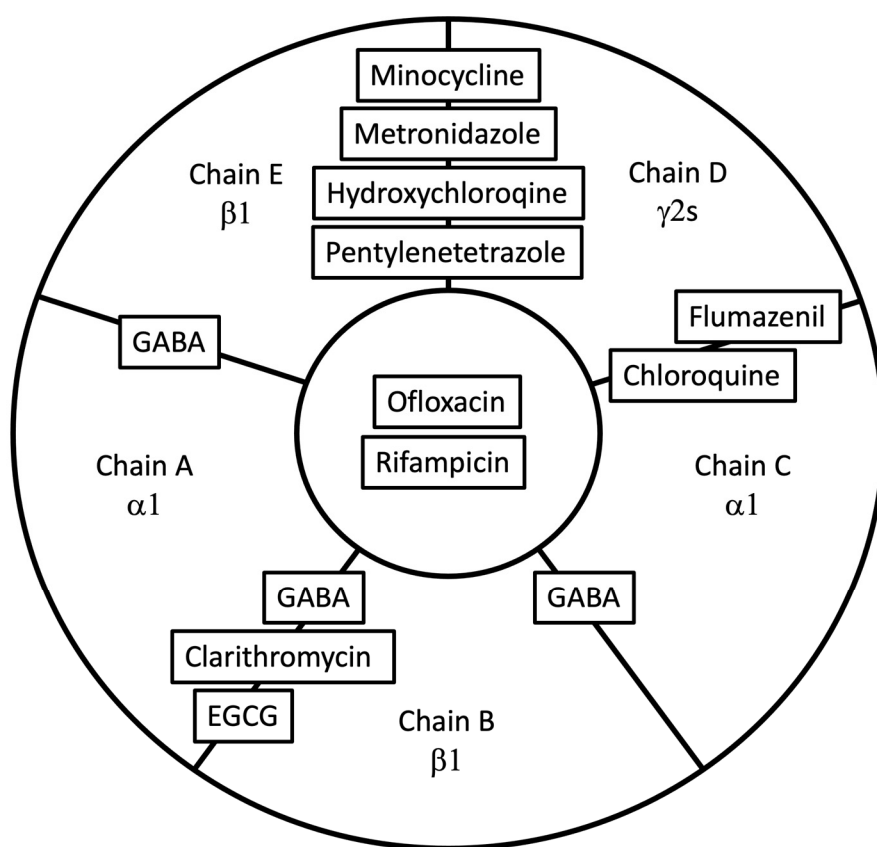


Figure 9. Cartoon of the predicted binding pockets of the compounds used in this study on the GABA_AR extracellular surface, as viewed from a synapse. No modulators were predicted to act at the 2 canonical ($\alpha\beta$) GABA binding sites. Clarithromycin and EGCG are predicted to act at the $\beta\alpha$ GABA binding site. Flumazenil and chloroquine both docked at the canonical benzodiazepine $\gamma\alpha$ binding site. Minocycline (data not shown), metronidazol, hydroxychloroquine, and pentylenetetrazole were all predicted to interact with the orphan $\beta\gamma$ binding site. Finally, ofloxacin and rifampicin were docked in the extracellular lumen.

5. Discussion

Our conventional and microfluidic electrophysiology experiments demonstrated that clarithromycin reduces GABA_AR activation and CSF-mediated potentiation. Our modeling studies suggest that it interacts with a distinct pocket on the receptor, previously thought to be an orphan site in GABA_ARs. Recently, the $\alpha^+\beta^-$ interface has been shown to contain electron density at saturating GABA concentrations that could order water, but more likely, a natural ligand [34]. If clarithromycin also binds at this location, it could act as a competitive GABA antagonist. If this is the case, we hypothesize that increasing the concentrations of clarithromycin would reduce the apparent affinity of the receptor for GABA limitlessly (or until the clarithromycin concentration reaches its solubility limit). Conversely, noncompetitive inhibition would produce a limited reduction in affinity, with receptor activation tending towards a finite GABA EC₅₀. To test this hypothesis, we constructed GABA concentration–function relationships in the presence of 0–300 μ M clarithromycin. The effect of clarithromycin concentration on GABA EC₅₀ is shown in Figure 10. Even as the clarithromycin concentration tended towards its aqueous solubility limit, the GABA EC₅₀ continued to increase. This reduction in apparent affinity suggests a competitive mechanism for clarithromycin, and support for the hypothesis that the $\alpha^+\beta^-$ pocket constitutes a third GABA binding site.

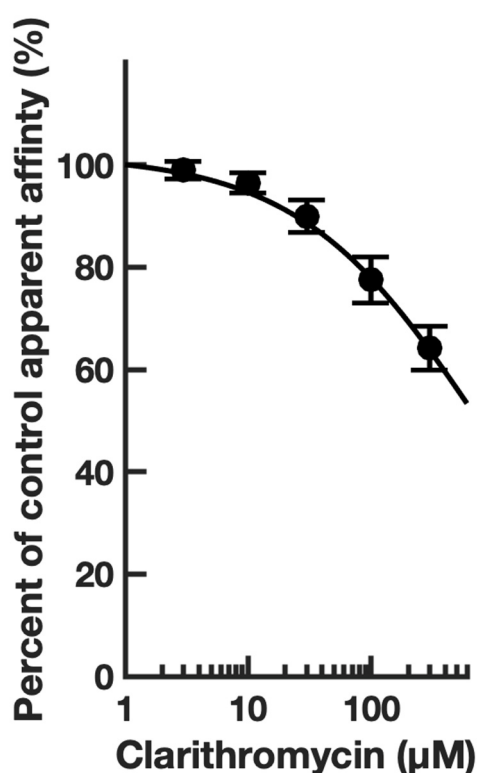


Figure 10. Increasing clarithromycin concentration raises the GABA EC₅₀ exponentially. The GABA EC₅₀ was determined at 6 different clarithromycin concentrations (0–300 μ M). The increase in EC₅₀ for each clarithromycin concentration is plotted as a decrease in apparent affinity.

Our data suggest that the chalate EGCG inhibits GABA activation and shares the $\alpha^+\beta^-$ GABA-binding pocket. Campbell et al. have also shown that EGCG blocks GABA activation [28]. In their detailed study, they show that the block is underpinned by an increase in the GABA EC₅₀. Taking these observations together, we hypothesize that the $\alpha^+\beta^-$ interface contains a functional GABA binding site that can be targeted by the competitive antagonists clarithromycin and EGCG. The GABA antagonist actions of these compounds are consistent with their use in humans, where they are both associated with increased arousal [9,10,29].

The convulsant pentylenetetrazole is a well-known GABA_AR blocker [46]. Its site and mechanism of action are equivocal. Early studies suggested an overlapping binding site with benzodiazepines [47]. This view changed to the general consensus that pentylenetetrazole is a channel blocker [48,49], and that it shares a transmembrane binding site with picrotoxin, which has now been resolved using cryo-electron microscopy [45]. However, the PTZ binding site consensus has been elegantly challenged [50], suggesting while there may be some overlap between the mechanisms of PTX and PTZ, the sites are distinct. Our findings support this latter finding. Using microfluidic patch clamp, we were able to demonstrate that PTZ was an effective inhibitor of GABA activation, and our modeling studies suggest that it does not prefer binding in the M2 2'-9' region of the channel, instead docking favorably in the orphan $\gamma^+\beta^-$ binding site. Interestingly, our structural models suggest that this site can also bind to the modest inhibitors metronidazole and hydroxychloroquine, and the irreversible blocker minocycline (data not shown).

Our findings have broader implication for the study of neuropharmacology and the treatment of patients with arousal disorders. In rat pyramidal neurons, clarithromycin has been shown to induce hyperexcitability, increase the firing rate, and reduce the amplitude of spontaneous miniature inhibitory postsynaptic GABAergic currents [51]. Our data strongly support these findings. Together, our work and previous studies suggest a mechanism of action for clarithromycin reversing sleepiness in patients suffering from idiopathic

hypersomnia. In this population, clarithromycin has been shown to improve subjective measures of sleep [9]. A recent meta-analysis of the available clinical data continues to favor the use of clarithromycin in the treatment of hypersomnia in the majority of cases [52].

Our clinical experience led us to investigate clarithromycin as a potential treatment for idiopathic hypersomnia, and as a potential novel GABA_AR-NAM. Since clarithromycin is not well-tolerated by many patients (the side effects include metallic taste, nausea, and headache), we sought to test other macrolides and antibiotics to see if they may also be useful in treating hypersomnia via a GABAergic mechanism. We were further motivated in this effort by the previous research into GABA_AR modulation by antibiotics from several drug classes, since many therapeutics used to treat infections are associated with disturbances in arousal [53,54]. For example, the β -lactam penicillin, is known to be a GABA_AR channel blocker [55], and quinolone antibiotics inhibit GABA receptor activation [56]. We were therefore hopeful that other macrolides and/or tetracyclines, ansamycins, etc., may demonstrate activity at the GABA_A receptor, and may represent additional therapeutic options for patients with poorly controlled excessive daytime sleepiness.

Our results with the quinolones chloroquine and hydroxychloroquine are consistent with this class of compounds having modest action at GABA_ARs. However, the prediction that the two chemically similar compounds prefer different binding pockets was not anticipated. Our studies indicate that the $\beta^- \gamma^+$ pocket can accommodate a diverse array of molecules, including hydroxychloroquine, yet chloroquine appears to prefer docking to the $\gamma^- \alpha^+$ pocket.

The promiscuous nature of the interactions predicted here is interesting and has been explored previously [57]. GABA_ARs contain a well-characterized agonist, GABAPAM and GABA_AR-NAM binding sites. The GABA and benzodiazepine agonist sites are found on either side of the alpha subunits (α^- and α^+ , respectively) while low-affinity GABAPAMs are thought to act at cavities between the helical transmembrane segments [45,58,59]. GABA_AR-NAMs seem to predominantly locate to the channel lumen. Our findings, while in part supporting this simple model, suggest that multiple sites, some novel, may play a role in receptor modulation and the side effects produced by the drugs studies here.

The clinical relevance of our findings are notable. With one exception (EGCG), the CNS concentration of the modulator is at least 37% of the GABA IC₅₀. Put another way, during normal therapeutic use, the compounds investigated here will have a significant effect on receptor activation in the CNS. Given the safety profile of these compounds, our findings suggest that some of these compounds might be useful in treating excessive sleepiness.

Finally, our studies have demonstrated that microfluidic patch clamp methods are a suitable substitute to conventional methods for screening GABA_A receptor modulators. We found that the microfluidic approach had several advantages over conventional methods. First, the apparatus is straightforward to use, and unlike conventional methods, it does not require prolonged training. Second, the miniaturized set-up means that drug or biological fluid use is reduced by 2–10-fold per data point. This is especially useful if screening small volumes of human samples, expensive therapeutics, or screening difficult-to-synthesize compounds. In fact, while each determination may need only 50 μ L of drug to set up the assay, after the experiment, 90% may be reclaimed for subsequent analysis. Third, the 384-well plate format facilitates the collection of large datasets (2000–4000 data episodes/hour). Finally, since the ensemble plate allows us to record from multiple cells simultaneously, this reduces the impact of cell–cell EC₅₀ variability. This is especially useful when studying allosteric modulators where strict adherence to a fixed reference of agonist is a critical part of the experimental design.

6. Conclusions

The compounds tested in this study are structurally diverse, yet they all modulate GABA_A receptor activation and can impair arousal in humans. From a structure–activity perspective, this may seem counterintuitive. Our modeling data provide an insight into this paradox, and show how the GABA_A receptor can act as a nexus for these compounds

by binding them at multiple sites that in turn, impair receptor activation, translating the binding of disparate molecular structures into changes in a common pathway.

Guided by the side effects associated with the therapeutics studies here, we have developed a pipeline of clinically safe compounds that may be useful in treating the symptoms of pathological sleepiness. These findings may benefit patients diagnosed with Idiopathic Hypersomnia, Type 1 Myotonic Dystrophy, or Kleine-Levin Syndrome, who experience excessive daytime sleepiness that is not controlled with conventional stimulants. Future work in human subjects and with human CSF samples are needed to determine the mechanisms of action and the therapeutic potential of these compounds.

Supplementary Materials: The following supporting information can be downloaded at: <https://www.mdpi.com/article/10.3390/biom13020365/s1>, Figure S1: Exemplar Ionflux Mercury current recording. Figure S2: Predicted binding pose for flumazenil. Figure S3: Detailed view of predicted binding poses for 10 compounds studied.

Author Contributions: Conceptualization, A.K., A.I.N., A.A.H.F., D.B.R., A.L.B. and A.J.; methodology, A.L.B. and A.J.; software, A.L.B. and A.J.; validation, A.K., A.A.H.F., L.G.L. and A.J.; formal analysis, A.J.; investigation, A.K., A.I.N., A.A.H.F., A.L.B., D.B.R. and L.G.L.; resources, D.B.R., A.L.B. and A.J.; data curation, A.J.; writing—original draft preparation, A.K., A.L.B. and A.J.; writing—review and editing, L.M.T., A.L.B. and A.J.; visualization, A.I.N., A.L.B. and A.J.; supervision, A.J.; project administration, A.J.; funding acquisition, D.B.R., L.M.T. and A.J. All authors have read and agreed to the published version of the manuscript.

Funding: Research reported in this publication was supported by the National Institutes of Neurological Disorders and Stroke of the National Institutes of Health under award number R01NS111280. The content is solely the responsibility of the authors and does not necessarily represent the official views of the National Institutes of Health.

Institutional Review Board Statement: Not applicable.

Informed Consent Statement: Not applicable.

Data Availability Statement: The data presented in this study are available on request from the corresponding author.

Conflicts of Interest: The authors declare no conflict of interest.

References

1. Fritschy, J.-M.; Mohler, H. GABAA-receptor heterogeneity in the adult rat brain: Differential regional and cellular distribution of seven major subunits. *J. Comp. Neurol.* **1995**, *359*, 154–194. [[CrossRef](#)] [[PubMed](#)]
2. Ehrlich, D.E.; Ryan, S.J.; Hazra, R.; Guo, J.D.; Rainnie, D.G. Postnatal maturation of GABAergic transmission in the rat basolateral amygdala. *J. Neurophysiol.* **2013**, *110*, 926–941. [[CrossRef](#)] [[PubMed](#)]
3. Yuan, H.; Low, C.-M.; Moody, O.A.; Jenkins, A.; Traynelis, S.F. Ionotropic GABA and Glutamate Receptor Mutations and Human Neurologic Diseases. *Mol. Pharmacol.* **2015**, *88*, 203–217. [[CrossRef](#)]
4. Gulinello, M.; Smith, S.S. Anxiogenic effects of neurosteroid exposure: Sex differences and altered GABAA receptor pharmacology in adult rats. *J. Pharmacol. Exp. Ther.* **2003**, *305*, 541–548. [[CrossRef](#)] [[PubMed](#)]
5. Majewska, M.D.; Harrison, N.L.; Schwartz, R.D.; Barker, J.L.; Paul, S.M. Steroid hormone metabolites are barbiturate-like modulators of the GABA receptor. *Science* **1986**, *232*, 1004–1007. [[CrossRef](#)] [[PubMed](#)]
6. Franks, N.P. General anaesthesia: From molecular targets to neuronal pathways of sleep and arousal. *Nat. Rev. Neurosci.* **2008**, *9*, 370–386. [[CrossRef](#)] [[PubMed](#)]
7. Rye, D.B.; Bliwise, D.L.; Parker, K.; Trott, L.M.; Saini, P.; Fairley, J.; Freeman, A.; Garcia, P.S.; Owens, M.J.; Ritchie, J.C.; et al. Modulation of vigilance in the primary hypersomnias by endogenous enhancement of GABAA receptors. *Sci. Transl. Med.* **2012**, *4*, 161ra51. [[CrossRef](#)] [[PubMed](#)]
8. Safavynia, M.S.A.; Keating, G.; Speigel, I.; Fidler, B.J.A.; Kreuzer, M.; Rye, M.D.B.; Jenkins, A.; García, M.P.S. Effects of gamma-Aminobutyric Acid Type A Receptor Modulation by Flumazenil on Emergence from General Anesthesia. *Anesthesiology* **2016**, *125*, 147–158. [[CrossRef](#)]
9. Trott, L.M.; Saini, P.; Bliwise, D.L.; Freeman, A.A.; Jenkins, A.; Rye, D.B. Clarithromycin in gamma-aminobutyric acid-Related hypersomnolence: A randomized, crossover trial. *Ann. Neurol.* **2015**, *78*, 454–465. [[CrossRef](#)]
10. Trott, L.M.; Saini, P.; Freeman, A.A.; Bliwise, D.L.; García, P.S.; Jenkins, A.; Rye, D.B. Improvement in daytime sleepiness with clarithromycin in patients with GABA-related hypersomnia: Clinical experience. *J. Psychopharmacol.* **2014**, *28*, 697–702. [[CrossRef](#)]

11. Lamp, K.C.; Freeman, C.D.; Klutman, N.E.; Lacy, M.K. Pharmacokinetics and Pharmacodynamics of the Nitroimidazole Antimicrobials. *Clin. Pharmacokinet.* **1999**, *36*, 353–373. [[CrossRef](#)]
12. Brown, R.; Price, R.J.; King, M.G.; Husband, A.J. Are antibiotic effects on sleep behavior in the rat due to modulation of gut bacteria? *Physiol. Behav.* **1990**, *48*, 561–565. [[CrossRef](#)] [[PubMed](#)]
13. Ahmed, A.; Misrani, A.; Tabassum, S.; Yang, L.; Long, C. Minocycline inhibits sleep deprivation-induced aberrant microglial activation and Keap1-Nrf2 expression in mouse hippocampus. *Brain Res. Bull.* **2021**, *174*, 41–52. [[CrossRef](#)] [[PubMed](#)]
14. Nonaka, K.; Nakazawa, Y.; Kotorii, T. Effects of antibiotics, minocycline and ampicillin, on human sleep. *Brain Res.* **1983**, *288*, 253–259. [[CrossRef](#)] [[PubMed](#)]
15. Jackson, M.L.; Butt, H.; Ball, M.; Lewis, D.P.; Bruck, D. Sleep quality and the treatment of intestinal microbiota imbalance in Chronic Fatigue Syndrome: A pilot study. *Sleep Sci.* **2015**, *8*, 124–133. [[CrossRef](#)] [[PubMed](#)]
16. Sarkar, S.; Khandelwal, S.K. Ofloxacin induced hypomania. *J. Clin. Diagn. Res.* **2013**, *7*, 1469–1470. [[CrossRef](#)]
17. Enginar, N.; Eroglu, L.; Ulak, G. The effect of ofloxacin on pentobarbital-induced sleep in mice. *Pharmacol. Biochem. Behav.* **1991**, *40*, 65–67. [[CrossRef](#)]
18. Akaike, N.; Shirasaki, T.; Yakushiji, T. Quinolones and fenbufen interact with GABA_A receptor in dissociated hippocampal cells of rat. *J. Neurophysiol.* **1991**, *66*, 497–504. [[CrossRef](#)]
19. Thompson, A.J.; Lummis, S.C.R. Antimalarial drugs inhibit human 5-HT(3) and GABA(A) but not GABA(C) receptors. *Br. J. Pharmacol.* **2008**, *153*, 1686–1696. [[CrossRef](#)]
20. Steere, A.C.; Angelis, S.M. Therapy for Lyme arthritis: Strategies for the treatment of antibiotic-refractory arthritis. *Arthritis Rheum.* **2006**, *54*, 3079–3086. [[CrossRef](#)]
21. Guan, P.; Sun, C.; Chen, Z.; Chen, J.; Ran, R. Long-term hydroxychloroquine therapy improves the quality of sleep in patients with primary Sjogren's syndrome: A real-world study. *Ann. Palliat. Med.* **2020**, *9*, 2203–2210. [[CrossRef](#)] [[PubMed](#)]
22. Trotti, L.M.; Saini, P.; Koola, C.; LaBarbera, V.; Bliwise, D.L.; Rye, D.B. Flumazenil for the Treatment of Refractory Hypersomnolence: Clinical Experience with 153 Patients. *J. Clin. Sleep Med.* **2016**, *12*, 1389–1394. [[CrossRef](#)]
23. De Deyn, P.P.; Marescau, B.; MacDonald, R.L. Epilepsy and the GABA-hypothesis a brief review and some examples. *Acta Neurol. Belg.* **1990**, *90*, 65–81. [[PubMed](#)]
24. Möhler, H. Cognitive enhancement by pharmacological and behavioral interventions: The murine Down syndrome model. *Biochem. Pharmacol.* **2012**, *84*, 994–999. [[CrossRef](#)]
25. Möhler, H. The legacy of the benzodiazepine receptor: From flumazenil to enhancing cognition in Down syndrome and social interaction in autism. *Adv. Pharmacol.* **2015**, *72*, 1–36. [[CrossRef](#)]
26. Rudolph, U.; Mohler, H. GABA_A receptor subtypes: Therapeutic potential in Down syndrome, affective disorders, schizophrenia, and autism. *Annu. Rev. Pharmacol. Toxicol.* **2014**, *54*, 483–507. [[CrossRef](#)] [[PubMed](#)]
27. Giménez, S.; Altuna, M.; Blessing, E.; Osorio, R.; Fortea, J. Sleep Disorders in Adults with Down Syndrome. *J. Clin. Med.* **2021**, *10*, 3012. [[CrossRef](#)]
28. Campbell, E.L.; Chebib, M.; Johnston, G.A. The dietary flavonoids apigenin and (-)-epigallocatechin gallate enhance the positive modulation by diazepam of the activation by GABA of recombinant GABA(A) receptors. *Biochem. Pharmacol.* **2004**, *68*, 1631–1638. [[CrossRef](#)] [[PubMed](#)]
29. Unno, K.; Pervin, M.; Nakagawa, A.; Iguchi, K.; Hara, A.; Takagaki, A.; Nanjo, F.; Minami, A.; Nakamura, Y. Blood–Brain Barrier Permeability of Green Tea Catechin Metabolites and their Neuritogenic Activity in Human Neuroblastoma SH-SY5Y Cells. *Mol. Nutr. Food Res.* **2017**, *61*, 1700294. [[CrossRef](#)]
30. Perszyk, R.E.; Yip, M.C.; McConnell, O.L.; Wang, E.T.; Jenkins, A.; Traynelis, S.F.; Forest, C.R. Automated Intracellular Pharmacological Electrophysiology for Ligand-Gated Ionotropic Receptor and Pharmacology Screening. *Mol. Pharmacol.* **2021**, *100*, 73–82. [[CrossRef](#)] [[PubMed](#)]
31. Dixon, C.; Sah, P.; Lynch, J.W.; Keramidas, A. GABA_A receptor alpha and gamma subunits shape synaptic currents via different mechanisms. *J. Biol. Chem.* **2014**, *289*, 5399–5411. [[CrossRef](#)] [[PubMed](#)]
32. Kallay, L.; Keskin, H.; Ross, A.; Rupji, M.; Moody, O.A.; Wang, X.; Li, G.; Ahmed, T.; Rashid, F.; Stephen, M.R.; et al. Modulating native GABA_A receptors in medulloblastoma with positive allosteric benzodiazepine-derivatives induces cell death. *J. Neurooncol.* **2019**, *142*, 411–422. [[CrossRef](#)] [[PubMed](#)]
33. Krummel, D.A.P.; Nasti, T.H.; Kaluzova, M.; Kallay, L.; Bhattacharya, D.; Melms, J.C.; Izar, B.; Xu, M.; Burnham, A.; Ahmed, T.; et al. Melanoma Cell Intrinsic GABA_A Receptor Enhancement Potentiates Radiation and Immune Checkpoint Inhibitor Response by Promoting Direct and T Cell-Mediated Antitumor Activity. *Int. J. Radiat. Oncol. Biol. Phys.* **2021**, *109*, 1040–1053. [[CrossRef](#)]
34. Phulera, S.; Zhu, H.; Yu, J.; Claxton, D.P.; Yoder, N.; Yoshioka, C.; Gouaux, E. Cryo-EM structure of the benzodiazepine-sensitive alpha1beta1gamma2S tri-heteromeric GABA(A) receptor in complex with GABA. *Elife* **2018**, *7*, e39383. [[CrossRef](#)] [[PubMed](#)]
35. Pervin, M.; Unno, K.; Takagaki, A.; Isemura, M.; Nakamura, Y. Function of Green Tea Catechins in the Brain: Epigallocatechin Gallate and its Metabolites. *Int. J. Mol. Sci.* **2019**, *20*, 3630. [[CrossRef](#)]
36. Osifo, N.G. The regional uptake of chloroquine in the rat brain. *Toxicol. Appl. Pharmacol.* **1979**, *50*, 109–114. [[CrossRef](#)]
37. Maniu, C.V.; Hellinger, W.C.; Chu, S.; Palmer, R.; Alvarez-Elcoro, S. Failure of Treatment for ChronicMycobacterium abscessus-Meningitis Despite Adequate Clarithromycin Levels in Cerebrospinal Fluid. *Clin. Infect. Dis.* **2001**, *33*, 745–748. [[CrossRef](#)]
38. Imshenetskaia, V.F. Erythromycin penetration into the cerebrospinal fluid of patients. *Antibiotiki* **1976**, *21*, 1002–1004.

39. Manzo, C.; Gareri, P.; Castagna, A. Psychomotor Agitation Following Treatment with Hydroxychloroquine. *Drug Saf. Case Rep.* **2017**, *4*, 6. [[CrossRef](#)]
40. Jokipii, A.M.M.; Myllylä, V.V.; Hokkanen, E.; Jokipii, L. Penetration of the blood brain barrier by metronidazole and tinidazole. *J. Antimicrob. Chemother.* **1977**, *3*, 239–245. [[CrossRef](#)]
41. Saivin, S.; Houin, G. Clinical Pharmacokinetics of Doxycycline and Minocycline. *Clin. Pharmacokinet.* **1988**, *15*, 355–366. [[CrossRef](#)] [[PubMed](#)]
42. Nau, R.; Kinzig, M.; Dreyhaupt, T.; Kolenda, H.; Sörgel, F.; Prange, H.W. Kinetics of ofloxacin and its metabolites in cerebrospinal fluid after a single intravenous infusion of 400 milligrams of ofloxacin. *Antimicrob. Agents Chemother.* **1994**, *38*, 1849–1853. [[CrossRef](#)] [[PubMed](#)]
43. Ramzan, I.M.; Levy, G. Kinetics of drug action in disease states. XIV. Effect of infusion rate on pentylenetetrazole concentrations in serum, brain and cerebrospinal fluid of rats at onset of convulsions. *J. Pharmacol. Exp. Ther.* **1985**, *234*, 624–628. [[PubMed](#)]
44. Ruiz-Bedoya, C.A.; Mota, F.; Tucker, E.W.; Mahmud, F.J.; Reyes-Mantilla, M.I.; Erice, C.; Bahr, M.; Flavahan, K.; de Jesus, P.; Kim, J.; et al. High-dose rifampin improves bactericidal activity without increased intracerebral inflammation in animal models of tuberculous meningitis. *J. Clin. Investig.* **2022**, *132*, e155851. [[CrossRef](#)]
45. Masiulis, S.; Desai, R.; Uchanski, T.; Martin, I.S.; Laverty, D.; Karia, D.; Malinauskas, T.; Zivanov, J.; Pardon, E.; Kotecha, A.; et al. GABA(A) receptor signalling mechanisms revealed by structural pharmacology. *Nature* **2019**, *565*, 454–459. [[CrossRef](#)] [[PubMed](#)]
46. Macdonald, R.L.; Barker, J.L. Pentylenetetrazole and penicillin are selective antagonists of GABA-mediated post-synaptic inhibition in cultured mammalian neurones. *Nature* **1977**, *267*, 720–721. [[CrossRef](#)]
47. Rehavi, M.; Skolnick, P.; Paul, S.M. Effects of tetrazole derivatives on [3H]diazepam binding in vitro: Correlation with convulsant potency. *Eur. J. Pharmacol.* **1982**, *78*, 353–356. [[CrossRef](#)]
48. Squires, R.F.; Saederup, E.; Crawley, J.N.; Skolnick, P.; Paul, S.M. Convulsant potencies of tetrazoles are highly correlated with actions on GABA/benzodiazepine/picrotoxin receptor complexes in brain. *Life Sci.* **1984**, *35*, 1439–1444. [[CrossRef](#)]
49. Ticku, M.K.; Maksay, G. Convulsant/depressant site of action at the allosteric benzodiazepine-gaba receptor-ionophore complex. *Life Sci.* **1983**, *33*, 2363–2375. [[CrossRef](#)]
50. Huang, R.Q.; Bell-Horner, C.L.; Dibas, M.I.; Covey, D.F.; Drewe, J.A.; Dillon, G.H. Pentylenetetrazole-induced inhibition of recombinant gamma-aminobutyric acid type A (GABA(A)) receptors: Mechanism and site of action. *J. Pharmacol. Exp. Ther.* **2001**, *298*, 986–995.
51. Bichler, E.K.; Elder, C.C.; García, P.S. Clarithromycin increases neuronal excitability in CA3 pyramidal neurons through a reduction in GABAergic signaling. *J. Neurophysiol.* **2017**, *117*, 93–103. [[CrossRef](#)] [[PubMed](#)]
52. Maski, M.K.; Trotti, L.M.; Kotagal, S.; Auger, R.R.; Swick, T.J.; Rowley, J.A.; Hashmi, M.S.D.; Watson, N.F. Treatment of central disorders of hypersomnolence: An American Academy of Sleep Medicine systematic review, meta-analysis, and GRADE assessment. *J. Clin. Sleep Med.* **2021**, *17*, 1895–1945. [[CrossRef](#)] [[PubMed](#)]
53. Grahl, J.J.; Stollings, J.L.; Rakshit, S.; Person, A.K.; Wang, L.; Thompson, J.L.; Pandharipande, P.P.; Ely, E.W.; Patel, M.B. Antimicrobial exposure and the risk of delirium in critically ill patients. *Crit. Care* **2018**, *22*, 337. [[CrossRef](#)] [[PubMed](#)]
54. Pejčić, A.V. Delirium associated with the use of macrolide antibiotics: A review. *Int. J. Psychiatry Clin. Pract.* **2022**, *26*, 29–42. [[CrossRef](#)]
55. Twyman, R.E.; Green, R.M.; MacDonald, R.L. Kinetics of open channel block by penicillin of single GABA_A receptor channels from mouse spinal cord neurones in culture. *J. Physiol.* **1992**, *445*, 97–127. [[CrossRef](#)]
56. Yakushiji, T.; Shirasaki, T.; Akaike, N. Non-competitive inhibition of GABA_A responses by a new class of quinolones and non-steroidal anti-inflammatories in dissociated frog sensory neurones. *Br. J. Pharmacol.* **1992**, *105*, 13–18. [[CrossRef](#)]
57. Koniuszewski, F.; Vogel, F.D.; Bampali, K.; Fabjan, J.; Seidel, T.; Scholze, P.; Schmiedhofer, P.B.; Langer, T.; Ernst, M. Molecular Mingling: Multimodal Predictions of Ligand Promiscuity in Pentameric Ligand-Gated Ion Channels. *Front. Mol. Biosci.* **2022**, *9*, 860246. [[CrossRef](#)]
58. Jenkins, A.; Andreasen, A.; Trudell, J.R.; Harrison, N.L. Tryptophan scanning mutagenesis in TM4 of the GABA(A) receptor alpha1 subunit: Implications for modulation by inhaled anesthetics and ion channel structure. *Neuropharmacology* **2002**, *43*, 669–678. [[CrossRef](#)]
59. Jenkins, A.; Greenblatt, E.P.; Faulkner, H.J.; Bertaccini, E.; Light, A.; Lin, A.; Andreasen, A.; Viner, A.; Trudell, J.R.; Harrison, N.L. Evidence for a common binding cavity for three general anesthetics within the GABA_A receptor. *J. Neurosci.* **2001**, *21*, RC136. [[CrossRef](#)]

Disclaimer/Publisher's Note: The statements, opinions and data contained in all publications are solely those of the individual author(s) and contributor(s) and not of MDPI and/or the editor(s). MDPI and/or the editor(s) disclaim responsibility for any injury to people or property resulting from any ideas, methods, instructions or products referred to in the content.